J Mol Model (2013) 19:1929–1936
DOI 10.1007/s00894-013-1758-3

ORIGINAL PAPER

First-principles vdW-DF investigation on the interaction between the oxazepam molecule and C_{60} fullerene

Masoud Darvish Ganji · Mahnaz Nashtahosseini · Saeed Yeganegi · Mahyar Rezvani

Received: 22 October 2012 / Accepted: 3 January 2013 / Published online: 24 January 2013
© Springer-Verlag Berlin Heidelberg 2013

Abstract The interaction between oxazepam and C_{60} fullerene was explored using first-principles vdW-DF calculations. It was found that oxazepam binds weakly to the fullerene cage via its carbonyl group. The binding of oxazepam to C_{60} is affected drastically by nonlocal dispersion interactions, while vdW forces affect the corresponding geometries only a little. Furthermore, aqueous solution affects the geometries of the oxazepam approaching to fullerene slightly, while oxazepam binds slightly farther away from the nanocage. The results presented provide evidence for the applicability of the vdW-DF method and serve as a practical benchmark for the investigation of host–guest interactions in biological systems.

Keywords Fullerenes · Drug delivery · Ab initio calculations · vdW-DF · Adsorption

Introduction

Novel drug delivery systems encompass new approaches to the delivery of drugs that address the limitations of traditional drug delivery systems. Nanoparticle-based drug delivery systems have considerable potential in the treatment of numerous illnesses [1, 2]. The essential technological characteristics of nanoparticles used as drug carriers are their high stability, high carrier capacity, and the possibility to incorporate both hydrophilic and hydrophobic substances. Nano- and micro-particles occupy a unique position in drug delivery technology due to their attractive properties. These can also be designed to allow controlled (sustained) drug release from the matrix. These properties of nanoparticles facilitate improvement of drug bioavailability and allow the reduction of dosing frequency [3, 4]. There are a number of studies on nanostructures and their ability to distribute peptides [5–7], DNA fragments [8], and other substances in vivo in biological systems, and preliminary results are encouraging [9–14]. Among nanomaterials, fullerenes—classes of nanosized structures made of networks of carbon atoms—are very attractive because of their unique properties and potential applications in electronics, materials science, and chemistry as well as in biochemistry and biology [15–23]. The remarkable mechanical and chemical stability of fullerenes makes them a promising nano-dimensional material for drug delivery applications. Since macroscopic samples of C_{60} became available in 1990, many applications have been suggested individually in the bio-area. Fullerenes and their derivatives have a range of medical applications, including as HIV inhibitor, photosensitive oxidizing factor against malignous skin cancer, or antioxidant activity healing neurodegenerative illnesses [24, 25].

Oxazepam [26, 27, 28] [serax; chemical name, (RS)-7-chloro-1,3-dihydro-3-hydroxy-5-2H-1,4-benzodiazepene-2, $C_{15}H_{11}Cl\,N_2O_2$] belongs to a group of drugs called benzodiazepines. Figure 1a shows a schematic representation of an oxazepam molecule. Oxazepam has been used extensively since the 1960s for the treatment of anxiety and insomnia and in the control of the symptoms of alcohol withdrawal. Oxazepam has moderate amnesic, anxiolytic, anticonvulsant, hypnotic, sedative and skeletal muscle-relaxant properties

M. D. Ganji (✉)
Department of Chemistry, Qaemshahr Branch,
Islamic Azad University, Qaemshahr, Iran
e-mail: ganji_md@yahoo.com

M. Nashtahosseini · S. Yeganegi
Faculty of Science, Department of Chemistry,
University of Mazandaran, Babulsar, Iran

M. Rezvani
Young Researchers Club, Central Tehran Branch, Department of Chemistry, Islamic Azad University, Tehran, Iran

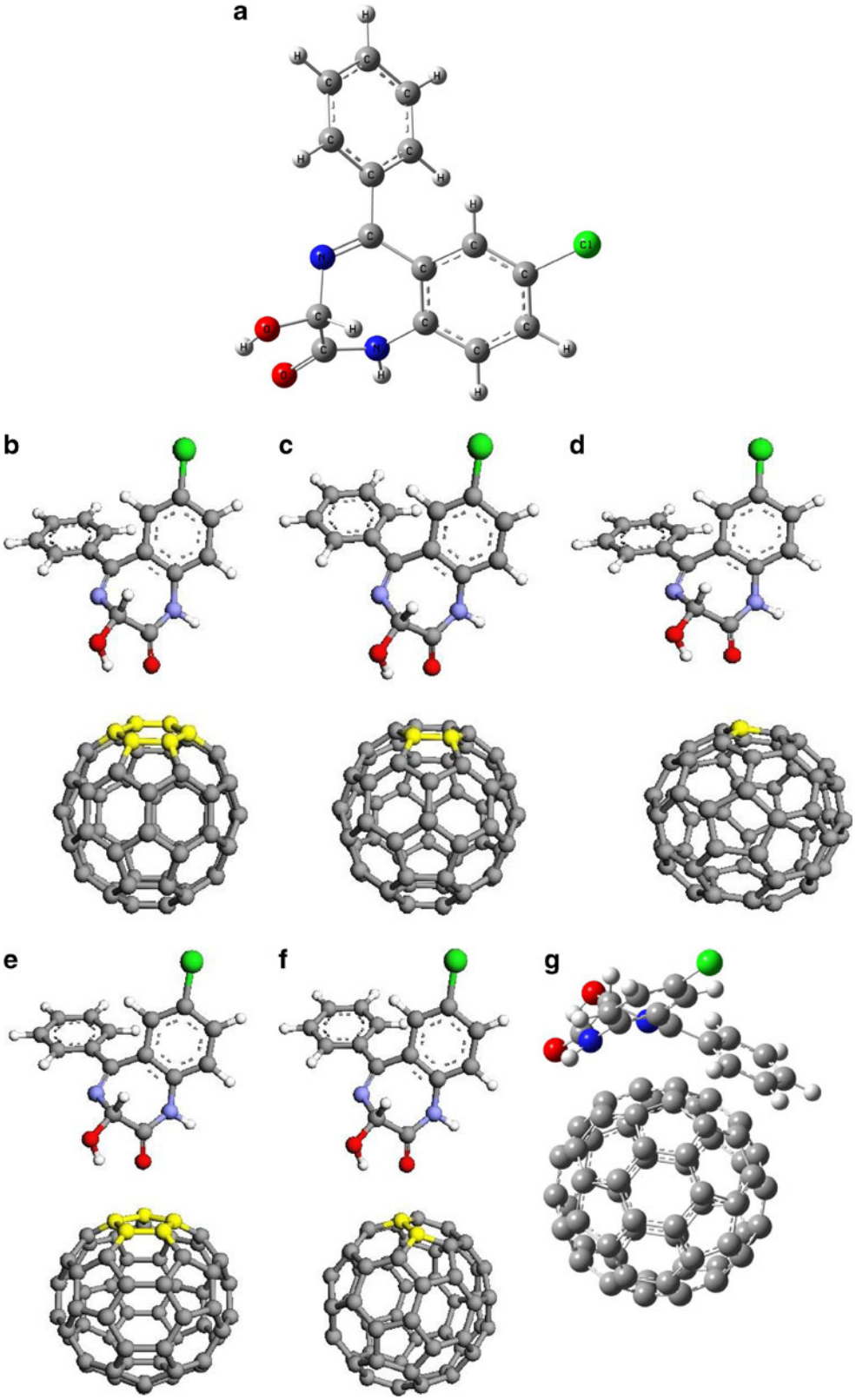

Fig. 1 **a** Structure of oxazepam. **b**–**f** Models of different adsorption states for oxazepam on the sidewall of the C_{60} fullerene on the six-membered (**b**) and five-membered (**c**) ring of the cage, the bridge sites above the C–C bonds (**d**, **e**) and the top site directly above the carbon top via its carbonyl oxygen (CO) active site (**f**). **g** Schematic representation of an oxazepam molecule approaching the fullerene side-wall through the aromatic-heterocyclic ring. The schemes are similarly orientated and were selected for oxazepam approaching the C_{60} nanocage via its hydroxyl oxygen (OH), chlorine (Cl) and hydroxyl oxygen (OH) active sites (not represented). Atom colors: *grey* carbon, *white* hydrogen, *blue* nitrogen, *green* chlorine, *red* oxygen

compared to other benzodiazepines. It is an intermediate acting benzodiazepine and acts on benzodiazepine-receptors resulting in increased effect of gamma-amino butyric acid (GABA) to the $GABA_A$ receptor, which results in inhibitory effects on the central nervous system. As oxazepam increases the activity of GABA in the brain, it increases its calming effect, resulting in sleepiness, a decrease in anxiety and relaxation of muscles.

In this work, we investigated the possibility of formation of a complex between fullerene C_{60} and oxazepam by using ab initio calculations based on density functional theory (DFT) methods [29]. We implemented first-principles calculations of the interaction between oxazepam and fullerene C_{60} to explain the possibility of formation of a stable complex. We show that it is important to include the nonlocal correlations responsible for long-range but strong van der Waals (vdW) interactions between the host and guest molecules. Furthermore, the role of vdW forces in aqueous solution was demonstrated explicitly. To evaluate the interaction between C_{60} and oxazepam, four active sites of oxazepam—the aromatic-heterocyclic ring, Cl, hydroxyl oxygen and carbonyl oxygen groups—as well as several sites of the fullerene C_{60} were considered. Details of the model as well as the computational methods employed are explained more thoroughly in the next section on Computational methods, followed by a discussion of our results in the Results and discussion, and a summary in the Conclusions.

Computational methods

We employed the *first-principles* approach using numerical atomic orbitals as the basis set with which to evaluate the structure and energy of the C_{60}-oxazepam complexes. We made use of generalized gradient approximation (GGA) [30, 31] with the Perdew-Burke-Ernzerhof (PBE) functional in DFT, and the standard norm-conserving Troullier-Martins pseudo-potentials [32]. We used the SIESTA code, which solves standard Kohn-Sham equations and has been established to be very efficient for large atomic systems.

The calculations were performed using a double-ζ basis composed of numerical atomic orbitals of finite range augmented by polarization functions (DZP) for all simulated atoms. The relaxed atomic structures of the systems considered were obtained by minimization of the total energy using Hellmann-Feynman forces including Pullay-like corrections. Structural optimizations were performed using the conjugate gradient algorithm until the residual forces were smaller than 0.02 eV Å $^{-1}$.

We also carried out calculations using the self-consistent implementation of the first-principles vdW density functional (vdW-DF) with a versatile real-space grid approach [33] employing long-range London dispersion corrections [34]. The vdW-DF was recently implemented in the SIESTA code and applied successfully to many systems [35–37]. We employed soft confinement potentials [38] to generate both double-ζ and triple-ζ plus polarization basis sets. We used an energy shift of 25 meV in each orbital in all calculations. Extensive examination indicated that this energy shift value provided good accuracy and ensures a large spatial extent of the basis orbitals, which is essential for preventing severe overestimation of binding [39, 40].

Results and discussion

To evaluate the binding energy between C_{60} and oxazepam, we first selected several configurations for the oxazepam molecule approaching different sites of the C_{60} cage skeleton. For this propose, we considered several sites in both the host and guest entities. Five and six-membered rings of the cage, the bridge sites above the C–C bonds, and the top site directly above the carbon atom (C-top) were chosen as selected sites for the C_{60} nanocage. For the oxazepam molecule, the Cl (halogen) atom, hydroxyl oxygen (OH), carbonyl oxygen (CO) and aromatic-heterocyclic ring were considered as selected sites for the active sites. For instance, the schematic representation of an oxazepam molecule approaching the considered chosen sites of the C_{60} nanocage via its carbonyl oxygen (CO) active site is shown in Fig. 1b–g. It should be mentioned that independently relaxed geometries for the fullerene and oxazepam molecules were used in the combined systems. We first performed vdW-DFT calculations on the considered systems. The calculated binding energies after full structural relaxation of the considered complexes indicate that the oxazepam prefers to be bound to the C_{60} via its carbonyl oxygen active site on the C atom of the nanocage.

The binding energy was obtained by using basis set super position error (BSSE) [41] correction via the formula:

$$E_{\mathrm{b}} = E(\mathrm{C_{60}} - \mathrm{oxaz}) - \left[E\left(\mathrm{C_{60ghost}} - \mathrm{oxaz}\right) + E\left(\mathrm{C_{60}} - \mathrm{oxaz_{ghost}}\right)\right]$$

Where the E (C_{60}-oxaz) is the total energy of the C_{60} interacting with the oxazepam. The 'ghost' molecule/C_{60} corresponds to additional basis wave functions centered at the position of the oxazepam or the C_{60}, but without any atomic potential.

The calculated binding energy and equilibrium distance between C atom of the C_{60} nanocage and carbonyl oxygen atom of the oxazepam in the stable configuration are about −0.14 eV (−3.23 kcalmol^{-1}) and 2.942 Å, respectively. It can be seen from the binding energy and equilibrium distance that a weak interaction (physisorption) exists between the oxazepam and C_{60} in the thermodynamically favorable complex [42–49]. The results obtained also show that the bond length of C–O in oxazepam extends to 1.233 Å, which is slightly longer than that in the isolated molecule (1.229 Å). The calculated adsorption energies for the most stable configurations of the other considered active sites are determined to be −0.13 eV for the Cl atom, −0.11 eV for the aromatic-heterocyclic group and −0.12 eV for OH active sites.

Electrostatic potential is well recognized as a factor that can explain and predict how simple molecules interact with other molecules [50–53]. The reactive site is a specifically charged area of a molecule that has an inclination to interact

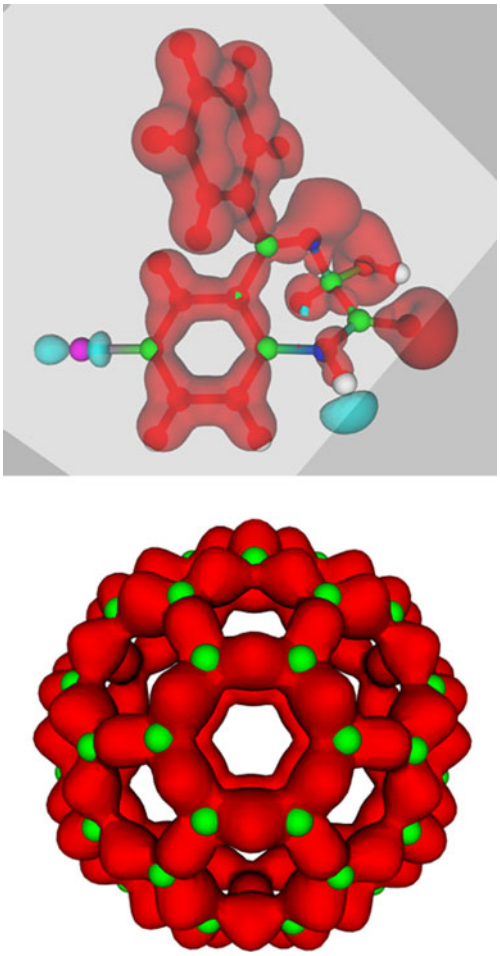

Fig. 2 Calculated electrostatic potential surface for an isolated oxazepam and C_{60} molecules at equilibrium geometry (isovalue set to 0.02). *Red* indicates an abundance of electrons (the lowest electrostatic potential energy), while *cyan* indicates a relative absence of electrons (the highest electrostatic potential energy)

with charged particles. Figure 2 presents an electrostatic diagram of interacting entities, i.e., C_{60} fullerene and oxazepam molecules). Oxygen has a higher electronegativity value than carbon hence oxygen atoms would accordingly have a higher electron density around them than carbon atoms (the sphere shaped objects surrounded by red regions in Fig. 2). It should be noted that the π regions of unsaturated portions of the molecules, i.e., aromatic rings, have a higher electron affinity than Cl atoms, thus the Cl atom sufferers a relative absence of electrons around it.

The electrostatic potential maps obtained for C_{60} fullerene show that there are regions with an abundance of electrons around C–C bonds. These are attributed to the π electrons and might be expected to be favorable sites for electrophilic attack but it is well recognized that the large electronegativity of C_{60} facilitates the transfer of electrons from the interacting species to the C_{60} nanocage [54]. Therefore, negative regions such as the oxygen atom of the oxazepam interact more strongly with C_{60} than the positively charged section (Cl atom) in the binding process.

To evaluate the basis set effects on the binding properties we also performed full structural geometry relaxation with the triple-ζ double polarized (TZDP) basis set for the most stable state. The results obtained reveal that the basis set only slightly affects the binding energy as well as the structural geometry of the considered system. The calculated binding energy and equilibrium distance between two nearest atoms from the host and guest molecules were determined to be −0.13 eV and 2.974 Å, respectively.

For comparison, a similar relaxation procedure was carried out for the considered systems within ordinary DFT calculations. The results obtained show that oxazepam prefers to be adsorbed on the C_{60} fullerene above the C atom with a binding energy of about −0.07 eV. We found that the binding energies of the oxazepam molecule to the C_{60} cage are affected significantly by the dispersion interaction. While the ordinary DFT predicts very weak binding, the dispersion interaction as implemented in the vdW-DF method changes this characteristic considerably. The binding energies obtained in ordinary DFT calculations are all lower than those obtained in vdW-DF calculations, with a difference of about 50 %.

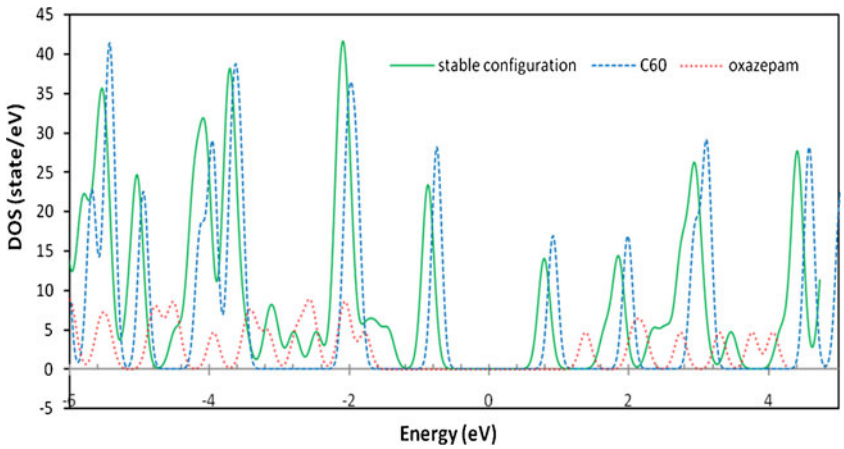

Fig. 3 Calculated density of states (DOS) for an isolated oxazepam, an isolated C_{60}, and the combination of the two at equilibrium geometry. The Fermi level was set at zero

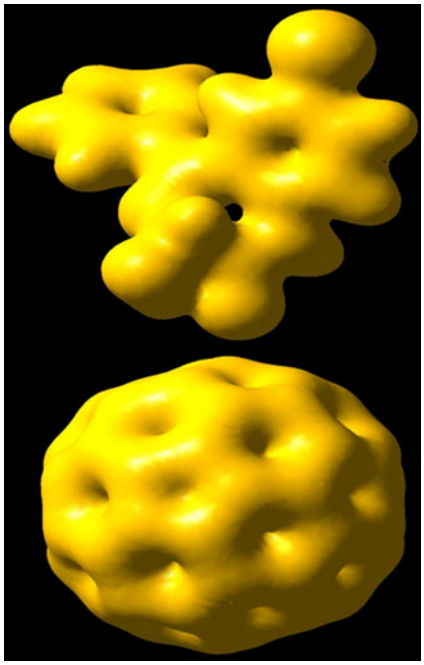

Fig. 4 Isosurface of the total electron density for oxazepam–C_{60} complexes where 0.02 was used as an isovalue of total electron density, showing the binding between C_{60} and the oxazepam molecule

In comparison with the PBE calculations, the vdW interaction was also found to affect the geometries of the oxazepam approaching to the fullerene nanocage only a little. The only difference was that the oxazepam bound slightly closer to the nanocage due to nonlocal vdW interaction. These results emphasize the importance of performing vdW interaction calculations of bio-molecules and nanostructures host-guest complexes.

To further interpret the nature of the binding in these systems, we study the electronic structures of the thermodynamically most stable state between oxazepam and C_{60}. For this purpose, the density of states (DOS) for the most stable configuration of the oxazepam-C_{60} complex was calculated (Fig. 3). As was clearly seen, there was no evidence for hybridization between the C_{60} and the oxazepam molecules, and the DOS near the Fermi level was not affected by the adsorption of oxazepam onto the cage. These results indicate that a small interaction was obtained quantitatively in terms of binding energies. Also, the minor difference in the Fermi level of the C_{60} (E_F=−4.03 eV) and oxazepam-C_{60} complex (E_F=−3.73 eV) clearly shows a weak charge transfer between the C_{60} and oxazepam in the adsorption process. Thus, we performed Mulliken charge analyses to estimate the amount of electron transfer between C_{60} and oxazepam. Charge analysis revealed a charge transfer of 0.03 *e* from oxazepam to the C_{60} cage skeleton for the most stable oxazepam-C_{60} complex, which confirms that a weak interaction (physisorption) takes place between the respective entities.

More insight can be gained from total electron density maps of the electronic densities. Figure 4 represents calculated isosurface maps for the most stable oxazepam–C_{60} complex. For the stable configuration, we find that the physically adsorbed oxazepam that is far from the cage has almost no effect on the electronic charge distribution of C atoms of the cage, and thus no charge transfer between the oxazepam and C_{60} molecular orbitals occurs.

In order to evaluate the weak interaction between the two reactants in the energetically favorable complex, we also calculated the highest occupied molecular orbital (HOMO) and lowest unoccupied molecular orbital (LUMO) electron density (Fig. 5). It is well known that the difference of the energies of the HOMO and LUMO (the band gap) can sometimes serve as a measure of the reactivity of the molecule. As can be seen from Fig. 5,

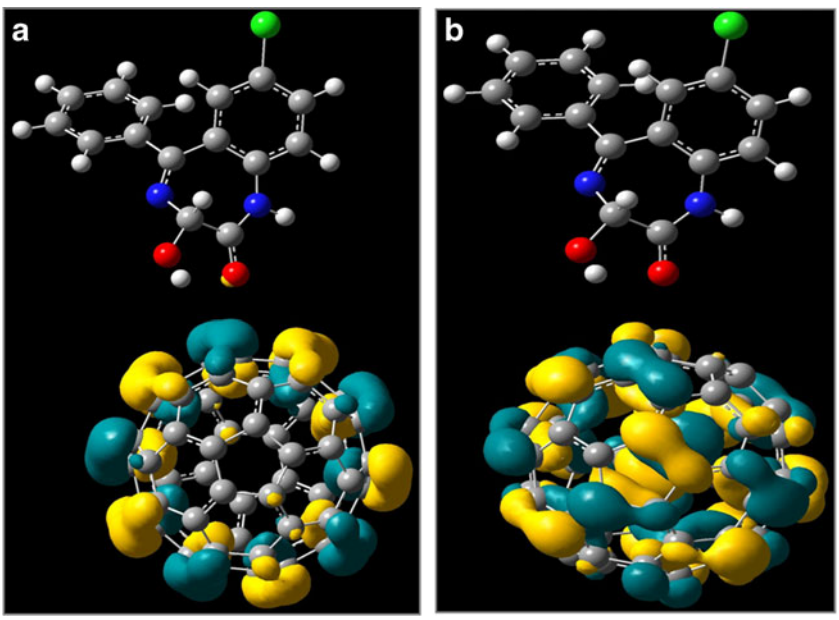

Fig. 5 Calculated orbitals localized at **a** the top-most valence band [highest occupied molecular orbital (HOMO)] and **b** the lowest conduction band [lowest unoccupied molecular orbital (LUMO)] of the C_{60} nanocage (the absolute values of the isosurfaces of the wave functions are 0.02). *Yellow* and *cyan* represent negative and positive regions of the wave functions, respectively

the HOMO and LUMO are located on the fullerene cage in the complex and nothing exists within the interacting distances. This highlights the weak interactions between oxazepam and C_{60} fullerene.

Next, we analyzed the DOS projected onto C and O atoms within the interacting distance, since this gives the most important information with respect to the orbitals involved in the adsorption process. The PDOS of the s orbital is just a mainly constant value over the whole range, thus is neglected here. Figure 6 shows the PDOS in arbitrary units around the Fermi energy for the C and O atoms of the C_{60} and oxazepam, respectively. It was found that both the HOMO and LUMO of the O and C atoms are more than 1.5 eV from the Fermi level and therefore does not lead to any bonding process in the adsorption. All the above calculations suggest that pristine C_{60} is not be a suitable material for oxazepam delivery, in the manner used for amino acids systems [55].

Finally, we evaluated solvent effects on the nature of binding of the host-guest complex as well as the corresponding geometries in aqueous solution. The relaxation was carried out

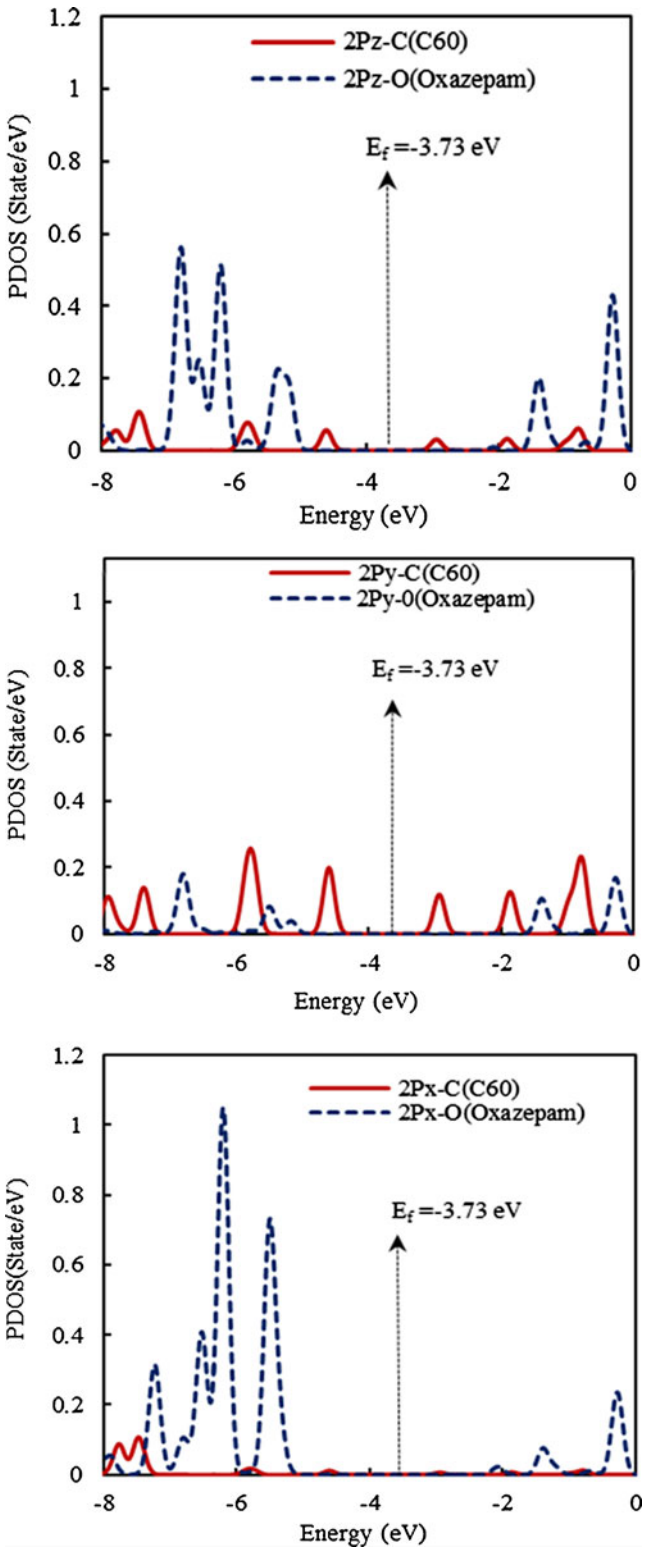

Fig. 6 Calculated partial density of states (PDOS) of C atom from the C_{60} and O atom for the most stable configuration. The energy at Fermi level is denoted by the dashed vertical line

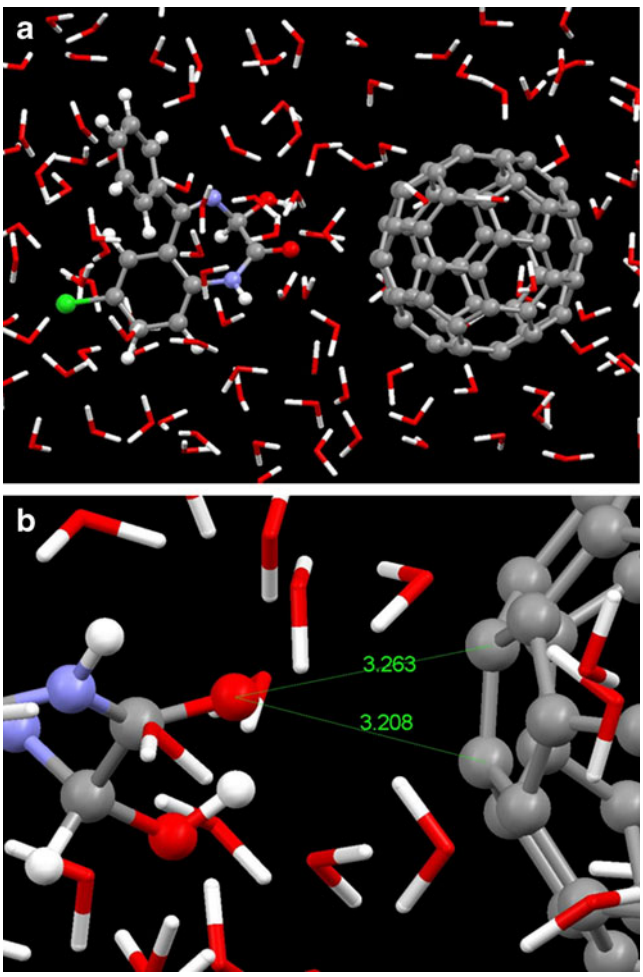

Fig. 7 Schematic representation of **a** simulation box filled with the most stable complex of oxazepam-fullerene and 110 water molecules, and **b** equilibrium distances between closest atoms from the interacting host–guest molecules in aqueous solution

in a rectangular box with periodic boundary conditions and filled with the most stable complex of oxazepam-fullerene and 110 water molecules, as shown in Fig. 7. The volume of the simulation box was assigned as $(17\times14\times20)$ Å^3. A full structural relaxation process was performed for the whole system under consideration. It was found that the aqueous solution affects the geometries of the oxazepam bound to the fullerene nanocage a little. The only difference was that the oxazepam bound slightly farther towards the nanocage due to the solvent effect. We also found that the O atom of the oxazepam moves toward the bridge site of the C–C bond with an average equilibrium distance of about 3.235 Å.

Conclusions

In summary, we have investigated the interaction between oxazepam and C_{60} fullerene using first-principles calculations based on vdW-DF methods. Several possible configurations were considered for the molecule approaching the side-wall of the fullerene nanocage, via their expected active sites. A full structural relaxation procedure was carried out for all the systems considered. The results obtained indicated that oxazepam binds to the side-wall of the cage through its carbonyl (-O) active site on the top of the C atom of the cage. However, the binding energy value (-3.23 kcal mol^{-1}) and equilibrium distance obtained from first-principles calculations is typical of physisorption.

Our results showed that the binding of oxazepam to the C_{60} nanocage is affected significantly by nonlocal dispersion interactions. It was also found that the vdW interaction affects the geometry of the oxazepam bounded to the nanocage slightly and that the oxazepam binds slightly closer to the nanocage surface due to vdW forces. A study of the electronic structure indicated that no significant hybridization between the respective orbitals of the host-guest molecules takes place, thus explaining the small interaction obtained quantitatively in terms of binding energies. In addition, only a weak charge transfer is observed between the fullerene cage and the oxazepam.

We further evaluated the effects of an aqueous environment on the binding properties and corresponding geometry of the most stable complex. Our first-principles results revealed that aqueous solution affects the geometries of the oxazepam approaching to fullerene nanocage only a little. The only difference is that the oxazepam bound slightly farther away from the nanocage due to the solvent effect and the O atom of the oxazepam was located above the bridge site of the C–C bond.

It is expected that the results presented here will help provide evidence for the applicability of the vdW-DF method and serve as a practical benchmark for the investigation of host–guest interacting systems in biological systems.

From the results obtained involving oxazepam, we can predict that typical drugs that contain chlorine, hydroxyl oxygen and carbonyl oxygen active sites might only form unstable binding with a C_{60} nanocage via their active sites.

References

1. Devi VK, Jain N, Valli KS (2010) Importance of novel drug delivery systems in herbal medicines. Pharmacogn Rev 4:27–31
2. Kshirsagar NA (2000) Drug delivery systems. Indian J Pharmacol 32:54–61
3. Diepold R, Kreuter J, Guggenbuhl P, Robinson JR (1989) Distribution of poly-hexyl-2-cyano-[3-^{14}C] acrylate nanoparticles in healthy and chronically inflamed rabbit eyes. Int J Pharm 54:149–153
4. Majeti NV, Ravi K (2000) Nano and microparticles as controlled drug delivery devices. J Pharm Pharm Sci 3:234–258
5. Jalbout AF, Jameel Hameed A, Jimenez-Fabian I, Ibrahim M, de Leon A (2008) Chalcanthrene-fullerene complexes: a theoretical study. J Organomet Chem 693:216–220
6. de Leon A, Jalbout AF, Basiuk VA (2008) SWNT-amino acid interactions: a theoretical study. Chem Phys Lett 457:185–190
7. Allen TM, Cullis PR (2004) Drug delivery systems: entering the mainstream. Science 303:1818–1822
8. Bianco A, Pantarotto D, Singh R, McCarthy D, Erhardt M, Briand JP, Parto M, Kostarelos K (2004) Functionalized carbon nanotubes for plasmid DNA gene delivery. Angew Chem Int Ed Engl 43 (39):5242–5246
9. Liu Z, Sun X, Nakayama-Ratchford N, Dai H (2007) Supramolecular chemistry on water-soluble carbon nanotubes for drug loading and delivery. ACS Nano 1:50–56
10. Kostarelos K, Bianco A, Prato M (2009) Promises, facts and challenges for carbon nanotubes in imaging and therapeutics. Nat Nanotechnol 4:627–633
11. Saikia N, Deka RC (2011) Density functional calculations on adsorption of 2 -methylheptylisonicotinate antitubercular drug onto functionalized carbon nanotube. Comp Theor Chem 964:257–261
12. de Menezes VM, Fagan SB, Zanella I, Mota R (2009) Carbon nanotubes interacting with vitamins: first principles calculations. Microelectron J 40:877–879
13. Guldi DM (2003) Molecular porphyrinfullerene architectures. Pure Appl Chem 75:1069–1075
14. Sinha R, Kim GJ, Nie S, Shin DM (2006) Nanotechnology in cancer therapeutics: bioconjugated nanoparticles for drug delivery. Mol Cancer Ther 5:1909–1917
15. Guldi DM, Prato M (2000) Excited-state properties of C (60) fullerene derivatives. Acc Chem Res 33:695–703
16. Jarvis SP, Uchihashi T, Ishida T, Tokumoto H, Nakayama Y (2000) Letter local solvation shell measurement in water using a carbon nanotube probe. J Phys Chem B 104:6091–6094
17. Kroto HW, Heath JR, O'Brien SC, Curl RF, Smalley RE (1985) C-60 Buckminsterfullerene. Nature 318:162–163
18. Zanella I, Fagan SB, Mota R, Fazzio A (2007) Ab initio study ofpristineand Si-doped capped carbon nanotubes interacting with nimesulide molecules. Chem Phys Lett 439:348–353
19. Castro Neto AH, Guinea F, Peres NMR, Novoselov KS, Geim AK (2009) The electronic properties of grapheme. Rev Mod Phys 81:109–162
20. Nakamura E, Isobe H (2003) Functionalized fullerenes in water. The first 10 years of their chemistry, biology, and nanoscience. Acc Chem Res 36:807–815

21. Hu YH, Ruckenstein E (2008) Complexes of a bio-molecule and a C60 cage. J Mol Struct THEOCHEM 850:67–71
22. de Menezes VM, Rocha AR, Zanella I, Mota R, Fazzio A, Fagan SB (2011) Electronic transport properties of ascorbic acid and nicotinamide adsorbed on single-walled carbon nanotubes. Chem Phys Lett 506:233–238
23. Boukhvalov DW, Katsnelson MI (2009) Chemical functionalization of grapheme. J Phys Condens Matter 21:344205–344226
24. Bianco A, Prato M (2003) Can carbon nanotubes be considered useful tools for biological applications? Adv Mater 15:1765–1768
25. Friedman SH, DeCamp DL, Sijbesma RP, Srdanov G, Wudl F, Kenyon GL (1993) Inhibition of the HIV-1 protease by fullerene derivatives: model building studies and experimental verification. J Am Chem Soc 115:6506–6509
26. Sieghart W (1994) Pharmacology of benzodiazepine receptors: an update. J Psychiatry Neurosci 19:24–29
27. Cameran A, Cameran N (1981) On the crystallography and stereochemistry of antiepileptic drugs. Acta Crystallogr B 37:1677–1679
28. Gilli G, Bertolasti V, Sacerdoti M, Borea PA (1978) The crystal and molecular structure of 7-chloro-1,3-dihydro-3-hydroxy-5-phenyl-2*H*-1,4-benzodiazepin-2-one (oxazepam). Acta Cryst B 34:2826–2829
29. Hohenberg P, Kohn W (1964) Inhomogeneous gas. Phys Rev 136:864–871
30. Langreth DC, Mehl MJ (1983) Beyond the local-density approximation in calculations of ground-state electronic properties. Phys Rev B 28:1809–1834
31. Perdew JP, Chevary JA, Vosko SH, Jackson KA, Pederson MR, Singh DJ, Fiolhais C (1992) Atoms, molecules, solids, and surfaces: applications of the generalized gradient approximation for exchange and correlation. Phys Rev B 46:6671–6687
32. Troullier N, Martins JL (1991) Efficient pseudopotentials for plane-wave calculations. Phys Rev B 43:1993–2006
33. Gulans A, Puska MJ, Nieminen RM (2009) Linear-scaling self-consistent implementation of the van der Waals density functional. Phys Rev B 79:201105–201109 (R)
34. Dion M, Rydberg H, Schröder E, Langreth DC, Lundqvist BI (2004) Van der Waals density functional for general geometries. Phys Rev Lett 92:246401–246404
35. Rydberg H, Dion M, Jacobson N, Schröder E, Hyldgaard P, Simak SI, Lungreth DC, Lundqvist BI (2003) Van der Waals density functional for layered structures. Phys Rev Lett 91:126402–126406
36. Johnston K, Kleis J, Lundqvist BI, Nieminen RM (2008) Influence of van der Waals forces on the adsorption structure of benzene on silicon studied using density functional theory. Phys Rev B 77:121404–121408 (R)
37. Román-Pérez G, Soler JM (2009) Efficient implementation of a van der Waals density functional: application to double-wall carbon nanotubes. Phys Rev Lett 103:096102–096106
38. Junquera J, Paz O, Sánchez-Portal D, Artacho E (2001) Numerical atomic orbitals for linear-scaling calculations. Phys Rev B 64:235111–235120
39. Rurali R, Lorente N, Ordejon P (2005) Molecular distortions and chemical bonding of a large pi-conjugated molecule on a metal surface. Phys Rev Lett 95:209601–209602
40. Hauschild A, Karki K, Cowie BCC, Rohlfing M, Tautz FS, Sokolowski M (2005) Hauschild et al. Reply. Phys Rev Lett 95:209602–209603
41. Boys SF, Bernardi F (1970) The calculation of small molecular interactions by the differences of separate total energies Some procedures with reduced errors. Mol Phys 19:553–566
42. Ganji MD (2009) First-principles simulation of the encapsulation of molecular hydrogen in C_{120} nanocapsules. Phys E 41:1433–1438
43. Ganji MD, Mohseni M, Goli O (2009) Modeling complexes of NH_3 molecules confined in C_{60} fullerene. J Mol Struct (THEOCHEM) 913:54–57
44. Ganji MD (2009) Density functional theory based treatment of amino acids adsorption on single-walled carbon nanotubes. Diam Relat Mater 18:662–668
45. Ganji MD (2008) Behavior of a single nitrogen molecule on the pentagon at a carbon nanotube tip: a first-principles study. Nanotechnology 19:025709–025714
46. Ganji MD (2008) Theoretical study of the adsorption of CO_2 on tungsten carbide nanotubes. Phys Lett A 372:3277–3282
47. Ganji MD, Rezvani M, Shokry M, Mirnejad A (2011) First-principles investigation on the formation of endohedral complexes between CH4 molecules and Si60 fullerene nanocage. Fullerenes Nanotubes Carbon Nanostruct 19:421–428
48. Ganji MD (2010) Calculations of encapsulation of amino acids inside the (13,0) single-walled carbon nanotube. Fullerenes Nanotubes Carbon Nanostruct 18:24–36
49. Ganji MD, Mirnejad A, Najafi A (2010) Theoretical investigation of methane adsorption onto boron nitride and carbon nanotubes. Sci Technol Adv Mater 11:045001–0450010
50. Murray JS, Seminario JM, Concha MC, Poltzer P (1992) An analysis of molecular electrostatic potentials obtained by a local density functional approach. Int J Quantum Chem 44:113–122
51. Murray JS, Riley KE, Politzer P, Clark T (2010) Directional weak intermolecular interactions: σ-hole bonding. Aust J Chem 63:1598–1607
52. Riley KE, Murray JS, Franfrlík J, Řezáč J, Solá RJ, Concha MC, Ramos RM, Politzer P (2011) Halogen bond tunability I: the effects of aromatic fluorine substitution on the strengths of halogen-bonding interactions involving chlorine, bromine, and iodine. J Mol Model 17:3309–3318
53. Poltzer P, Riley KE, Bulat FA, Murray JS (2012) Perspectives on halogen bonding and other σ-hole interactions: *Lex parsimoniae* (Occam's Razor). Comp Theor Chem 998:2–8
54. Sun Q, Wang Q, Jena P, Kawazoe Y (2005) Clustering of Ti on a C60 surface and its effect on hydrogen storage. J Am Chem Soc 127:14582–14583
55. Ganji MD, Yazdani H, Mirnejad A (2010) $B_{36}N_{36}$ Fullerene-like nanocages: a novel material for drug delivery. Phys E 42:2184–2189